Journal of Electrochemistry

Volume 29
Issue 6 *Special Issue on Interfactial Regulation and Electrochemical sensors*

2023-06-28

Boronate Affinity-Assisted Electrochemically Controlled ATRP for Ultrasensitive Electrochemical Aptasensing of Carcinoembryonic Antigen

Qiong Hu
Guangzhou Key Laboratory of Sensing Materials and Devices, Center for Advanced Analytical Science, School of Chemistry and Chemical Engineering, Guangzhou University, Guangzhou 510006, Guangdong, P. R. China, q.hu@gzhu.edu.cn

Shi-Qi Li

Yi-Yi Liang

Wen-Xing Feng

Yi-Lin Luo

Xiao-Jing Cao

Li Niu
Guangzhou Key Laboratory of Sensing Materials and Devices, Center for Advanced Analytical Science, School of Chemistry and Chemical Engineering, Guangzhou University, Guangzhou 510006, Guangdong, P. R. China, lniu@gzhu.edu.cn

Recommended Citation

Qiong Hu, Shi-Qi Li, Yi-Yi Liang, Wen-Xing Feng, Yi-Lin Luo, Xiao-Jing Cao, Li Niu. Boronate Affinity-Assisted Electrochemically Controlled ATRP for Ultrasensitive Electrochemical Aptasensing of Carcinoembryonic Antigen[J]. *Journal of Electrochemistry*, 2023 , 29(6): 2218001.
DOI: 10.13208/j.electrochem.2218001
Available at: https://jelectrochem.xmu.edu.cn/journal/vol29/iss6/14

ARTICLE

Boronate Affinity-assisted Electrochemically Controlled ATRP for Ultrasensitive Electrochemical Aptasensing of Carcinoembryonic Antigen

Qiong Hu*, Shi-Qi Li, Yi-Yi Liang, Wen-Xing Feng, Yi-Lin Luo, Xiao-Jing Cao, Li Niu*

Guangdong Engineering Technology Research Center for Sensing Materials and Devices, Guangzhou Key Laboratory of Sensing Materials and Devices, Center for Advanced Analytical Science, School of Chemistry and Chemical Engineering, Guangzhou University, Guangzhou, 510006, PR China

Abstract

As an acidic glycoprotein, carcinoembryonic antigen (CEA) is of great value as a broad-spectrum tumor marker in the differential diagnosis and surveillance of malignant tumors. In this work, we report an electrochemical aptasensor for the ultrasensitive and highly selective detection of CEA, taking advantage of the dual amplification by the boronate affinity-assisted electrochemically controlled atom transfer radical polymerization (BA-eATRP). Specifically, the BA-eATRP-based electrochemical aptasensing of CEA involves the capture of target antigens by nucleic acid aptamers, the covalent crosslinking of ATRP initiators to CEA antigens via the selective interactions between the phenylboronic acid (PBA) group and the *cis*-diol group of the monosaccharide residues, and the collection of the ferrocene (Fc) reporters via the eATRP of ferrocenylmethyl methacrylate (FcMMA). As CEA is decorated with hundreds of *cis*-diol groups, the BA-based crosslinking can result in the labeling of each CEA with hundreds of ATRP initiators; furthermore, the eATRP of FcMMA results in the surface-initiated growth of long-chain ferrocenyl polymers, leading to the tethering of each ATRP initiator-conjugated site with hundreds to thousands of Fc reporters. Such that, the BA-eATRP can result in the efficient labeling of each CEA with a plenty of Fc reporters. Under the optimized conditions, the BA-eATRP-based strategy enables the highly selective aptasensing of CEA at a concentration as low as 0.34 pg·mL^{-1}, with a linear range of 1.0−1000 pg·mL^{-1}. Besides, this aptasensor has been successfully applied to the quantitative analysis of CEA in human serum. The BA-eATRP-based electrochemical aptasensor is cost-effective and simple in operation, holding broad application prospect in the ultrasensitive and highly selective detection of CEA.

Keywords: Boronate affinity; Atom transfer radical polymerization; Electrochemical aptasensor; Carcinoembryonic antigen; Tumor marker; Signal amplification

1. Introduction

Carcinoembryonic antigen (CEA) is a cell adhesion-related acidic glycoprotein [1]. As a oncofetal antigen, CEA is normally secreted by the gastrointestinal tissue during fetal development and occurs at very low levels in the serum of healthy adults [1]. However, the level of CEA is often elevated in the serum of individuals suffering from various neoplastic conditions (e.g., colorectal cancer, gastric cancer, pancreatic cancer, lung cancer, breast cancer, and medullary thyroid cancer) [2] and some non-neoplastic conditions (e.g., cirrhosis, pancreatitis, ulcerative colitis, hypothyroidism, and Crohn's disease) [3]. Due to the poor sensitivity and specificity, CEA is unable to act as a tumor marker for the diagnosis and screening of a specific cancer. However, it is of great value as a broad-spectrum tumor marker in the differential diagnosis and surveillance of malignant tumors [1,4]. As the cutoff value of CEA for clinical application is 5 ng·mL^{-1} [5], sensitive and selective detection of CEA is highly desired.

In recent decades, a diversity of methods have already been established for CEA detection, such as fluorescent [6,7], photoelectrochemical (PEC)

Received 5 August 2022; Received in revised form 8 September 2022; Accepted 15 September 2022
Available online 19 September 2022

* Corresponding author, Qiong Hu, Tel: (86)15850560755, E-mail address: q.hu@gzhu.edu.cn.
* Corresponding author, Li Niu, Tel: (86)15915778899, E-mail address: lniu@gzhu.edu.cn.

https://doi.org/10.13208/j.electrochem.2218001

[8−10], surface-enhanced Raman scattering (SERS) [11,12], colorimetric [13,14], electrochemiluminescent [15−18], and electrochemical biosensors [19−21], using such as antibodies [22,23], imprinted polymers [24,25], and aptamers [26−28] as the capture elements. Among them, electrochemical aptasensing of CEA has attracted much attention by virtue of the advantages of low detection cost, minimal matrix/background interference, simple instrument, and high sensitivity and selectivity [29,30]. Nevertheless, most of the previously developed electrochemical CEA aptasensors necessitated the use of sophisticated enzymatic reactions (e.g., DNAzymes) [31,32] or nanocomposites (e.g., nanoclusters) [33,34] for signal amplification, which is not practical for clinical applications.

By virtue of the simplicity, high efficiency, and cost-effectiveness, the grafting of polymer chains through reversible deactivation radical polymerization, such as atom transfer radical polymerization (ATRP) [35,36] and reversible addition-fragmentation chain-transfer (RAFT) polymerization [37,38], has attracted growing attention as an amplification strategy in the sensitive detection of biotargets [39,40]. Among them, ATRP involves the use of the alkyl halide initiators (R-X) and the lower oxidation state transition-metal activators (typically the Cu(I) complexes) [41,42]. Specifically, reduction of the initiators by the activators generates the radical species, which then react with monomers to form long-chain polymers [42]. In the electrochemically controlled ATRP (eATRP), the Cu(I) activators are generated from the electrochemical reduction of the Cu(II) deactivators [43], holding the merits of the improved control over polymer growth, better biocompatibility, and higher O_2 tolerance [40,44].

On the basis of the dual amplification by the boronate affinity (BA)-assisted eATRP (BA-eATRP), we report herein a cost-effective and easy-to-operate electrochemical aptasensor for the ultrasensitive and highly selective detection of CEA. As the capture elements, the DNA aptamers were attached to a gold electrode via the gold-sulfur self-assembly chemistry. After the capture of CEA antigens, the oligosaccharide chains of CEA were leveraged for the covalent crosslinking of ATRP initiators via the selective interactions between the phenylboronic acid (PBA) group and the *cis*-diol group of the monosaccharide residues [45,46]. Further, potentiostatic reduction of the Cu(II) deactivators resulted in the generation of the Cu(I) activators [40,44], triggering the eATRP of ferrocenylmethyl methacrylate (FcMMA) and thus the surface-initiated growth of long-chain ferrocenyl polymers. As each CEA is decorated with hundreds of *cis*-diol groups for the BA-based crosslinking of ATRP initiators while each ATRP initiator-conjugated site can be tethered with hundreds to thousands of Fc reporters, the BA-eATRP can result in the labeling of each CEA with a plenty of Fc reporters. As a result, the BA-eATRP-based electrochemical CEA aptasensor is highly sensitive and selective. Moreover, it is cost-effective and east-to-operate, thus holding great promise in clinical applications.

2. Experimental

2.1. BA-eATRP-based electrochemical aptasensing of CEA

Prior to use, gold electrode (Au) was cleaned as described elsewhere [47,48]. After incubating the Au with 10 μL of 0.5 $\mu mol \cdot L^{-1}$ aptamer (Apt, 10 $mmol \cdot L^{-1}$ NaH_2PO_4/Na_2HPO_4 (PBS, pH7.4)) at 37 °C for 30 min, the Apt/Au was rinsed with ultrapure H_2O, incubated with 6-mercapto-1-hexanol (MH, 1.0 $mmol \cdot L^{-1}$ in 60% ethanol) at 37 °C for 15 min, and rinsed with ethanol and ultrapure H_2O. After incubating the MH/Apt/Au with 10 μL of CEA (10 $mmol \cdot L^{-1}$ PBS, pH7.4) at 37 °C for 45 min, the CEA/MH/Apt/Au was rinsed with ultrapure H_2O, incubated with (4-(2-bromo-2-phenylacetylamino)phenyl)boronic acid (PBABr, 0.5 $mmol \cdot L^{-1}$ in 10 $mmol \cdot L^{-1}$ PBS containing 10% DMF (pH9.5)) at 37 °C for 15 min, and rinsed with ethanol and ultrapure H_2O. The PBABr/CEA/MH/Apt/Au was soaked into the polymerization solution (obtained by adding 0.1 mL of FcMMA (10 $mmol \cdot L^{-1}$ in DMF), 0.1 mL of $Cu^{II}Br/Me_6TREN$ (10 $mmol \cdot L^{-1}$ in H_2O), 7.5 mL of KPF_6 (0.1 $mol \cdot L^{-1}$), and 1.0 mL of KBr (1.0 $mol \cdot L^{-1}$) into 1.3 mL of DMF), followed by the eATRP of FcMMA at room temperature (ca. 25 °C) for 40 min using *i-t* curve. After removal of the possible Cu(0) residues via the anodic oxidation at 0.19 V (*vs.* saturated calomel electrode (SCE)) for 30 s, the Fc/PBABr/CEA/MH/Apt/Au was tested by square wave voltammetry (SWV; potential increase, 4.0 mV; potential amplitude, 25 mV; frequency, 15 Hz) in 0.5 $mol \cdot L^{-1}$ $LiClO_4$ [47,48].

3. Results and discussion

3.1. Principle of the BA-eATRP-based electrochemical CEA aptasensor

The principle of the electrochemical CEA aptasensor is shown in Scheme 1. The aptamer was used as the recognition element and it was tethered via the Au-S chemistry. As CEA is a glycoprotein

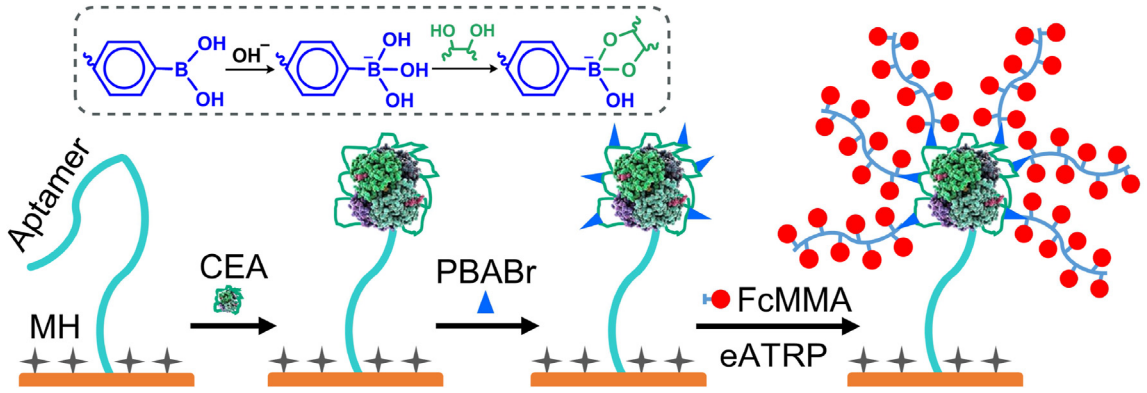

Scheme 1. Principle of the BA-eATRP-based electrochemical CEA aptasensor.

[49], the ATRP initiators for the later polymerization were covalently crosslinked to the aptamer-captured antigens via the facile, selective interactions between the *cis*-diol groups of the monosaccharide residues and the PBA group [50–52]. Afterward, the eATRP of FcMMA resulted in the surface-initiated growth of the Fc-conjugated polymer chains and consequently the collection of Fc reporters [48]. As each CEA is decorated with hundreds of *cis*-diol groups for the BA-based crosslinking of ATRP initiators while each long-chain polymer can be composed of a plenty of Fc reporters, the BA-eATRP enabled the dual-amplification detection. Thus, the BA-eATRP-based electrochemical CEA aptasensor is ultrasensitive and highly selective.

3.2. Effect of eATRP potential

The surface-initiated growth of the Fc-conjugated polymer chains via the eATRP of FcMMA was initiated and sustained through the electrochemical reduction of the Cu(II) deactivators. With this in mind, the redox properties of the Cu(II) deactivator were investigated. As displayed in Fig. 1A, the cyclic voltammetric (CV) curve of the Cu(II) deactivator at the PBABr/CEA/MH/Apt/Au presented a reduction peak at −0.58 V, corresponding to the reduction of the Cu(II) deactivators into the Cu(I) activators [43,44]. For the [Cu^{II}Br/L]/[Cu^{I}/L] redox couple (L = Me_6TREN), the Nernst equation can be expressed as $E_{app} = E^{o'} + (RT/nF) * \ln\{[Cu^{II}Br/L]/[[Cu^{I}/L] * [Br^{-}]]\}$. It is obvious that the concentration of the Cu(I) activator is highly dependent on the eATRP potential (E_{app}) [43,44]. Specifically, a higher E_{app} would result in a lower concentration of the Cu(I) activator, while a more negative E_{app} would result in the generation of more Cu(I) activators [43]. As the initiating radicals ($R^{\bullet}$) were generated from the reduction of the ATRP initiators by the Cu(I) activators [43], the rate of the surface-initiated growth of polymer chains was dependent on the E_{app} [43,44]. With this in mind, the effect of eATRP potential on the detection signal was investigated. The peak current corresponding to the anodic oxidation of the Fc reporters, as displayed in Fig. 1B, exhibited the highest value at the eATRP potential of −0.54 V,

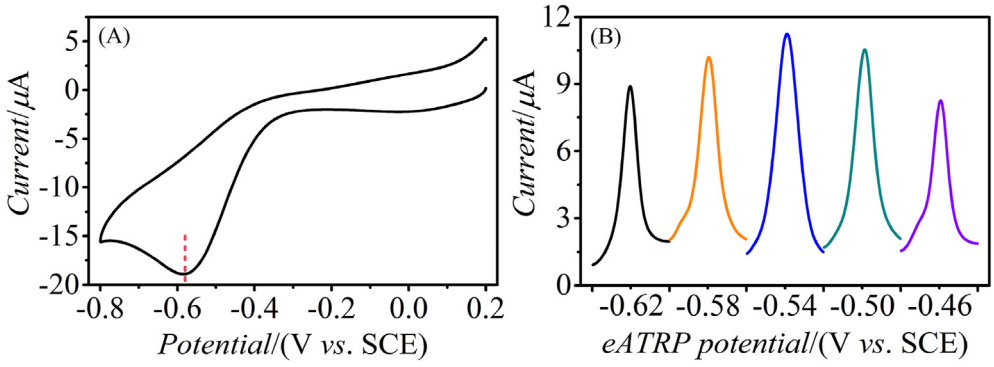

Fig. 1. (A) CV curve of the PBABr/CEA/MH/Apt/Au in the FcMMA-free polymerization solution (the dashed vertical line indicates the reduction peak). (B) Effect of eATRP potential on the detection signal. CEA, 1.0 ng·mL^{-1}.

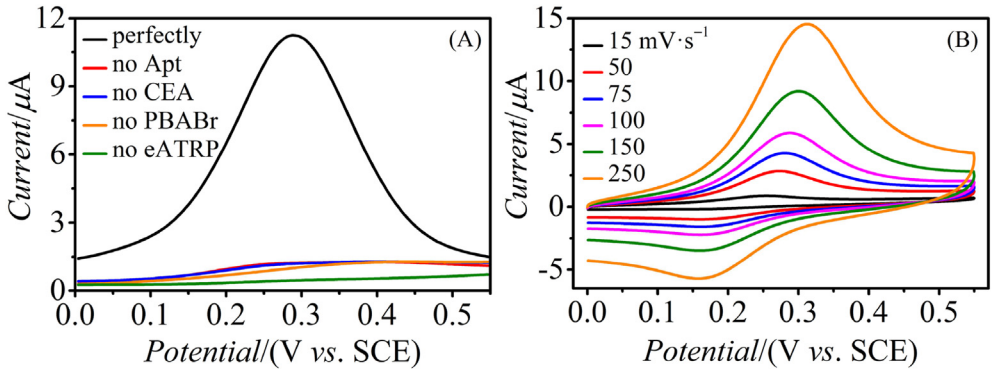

Fig. 2. (A) SWV curves of various electrodes. (B) CV curves of the Fc/PBABr/CEA/MH/Apt/Au at various scan rates. CEA, 1.0 ng·mL^{-1}.

which was hence adopted in the subsequent experiments.

3.3. Characterizations of the electrochemical CEA aptasensor

The feasibility of the BA-eATRP-based electrochemical CEA aptasensor was investigated based on the SWV curves derived from various electrodes. As seen in Fig. 2A, the perfectly modified electrode (i.e., the Fc/PBABr/CEA/MH/Apt/Au) can be featured by a high oxidation peak at ca. 0.29 V, while no oxidation peak could be observed for the PBABr/CEA/MH/Apt/Au (i.e., without eATRP). This observation validated that the oxidation current observed at ca. 0.29 V was derived from the electrochemical oxidation of the Fc reporters. Likewise, almost no oxidation peak could be observed for the electrodes modified in the absences of aptamers, CEA antigens, or the PBABr agents. The high reliability of the detection signal validated the feasibility of the BA-eATRP-based electrochemical CEA aptasensor. CV of the Fc/PBABr/CEA/MH/Apt/Au was further applied to investigate the redox behavior of the Fc reporters (Fig. 2B). As the Fc reporters were surface-tethered, the peak currents showed well-defined linear correlation with the scan rate (Figure S1), confirming the surface-confined charge-transfer process [47,48]. Fig. 3 clearly shows that there is a high density of polymer chains on the Fc/PBABr/CEA/MH/Apt/Au. Apart from the P elements observed for the DNA aptamer in the energy dispersive X-ray spectrum (EDS) mapping as shown in Fig. 4A, the EDS mappings of the B (Fig. 4B) and Br elements (Fig. 4C) proved the presence of PBABr, while that of the Fe element (Fig. 4D) unequivocally demonstrated the presence of the Fc reporters.

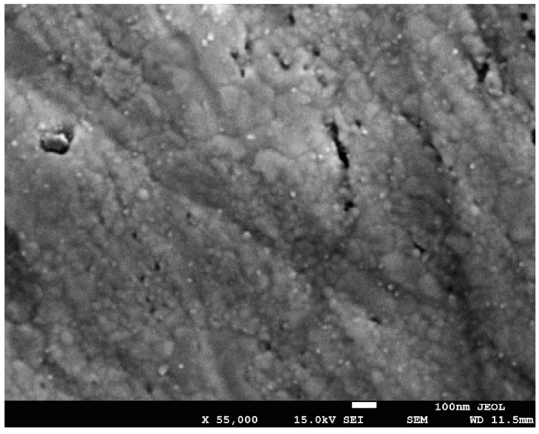

Fig. 3. SEM image of the Fc/PBABr/CEA/MH/Apt/Au. CEA, 1.0 ng·mL^{-1}.

The preparation of the Fc/PBABr/CEA/MH/Apt/Au was monitored by electrochemical impedance spectroscopy (EIS, Fig. 5A) and CV (Fig. 5B). For the Au, the charge-transfer resistance (R_{ct}) was the smallest (Fig. 5A,a), while the redox currents were the highest (Fig. 5B,a). Owing to the steric hindrance of the aptamer layer, and the electrostatic repulsion between the phosphate groups and the $[Fe(CN)_6]^{3-/4-}$ [44], the modification of aptamers (i.e., the Apt/Au) resulted in the increase of the R_{ct} (Fig. 5A and b) and the decrease of the redox currents (Fig. 5B,b). As the blocking of the residual sites would cause an increase in the steric hindrance [43,47], the MH/Apt/Au showed a higher R_{ct} (Fig. 5A,c) and the lower redox currents (Fig. 5B and c) relative to the Apt/Au. As displayed, the capture of CEA antigens by aptamers (i.e., the CEA/MH/Apt/Au) resulted in a slightly increased R_{ct} (Fig. 5A,d) and slightly decreased redox currents (Fig. 5B,d) [45,46]. As the affinity crosslinking between the *cis*-diol groups and the PBA groups resulted in the formation of the negatively-charged phenylborates [53,54], the PBABr/CEA/MH/Apt/Au featured a significantly increased R_{ct} (Fig. 5A,e) and significantly decreased redox currents (Fig. 5B,e) relative to the CEA/MH/Apt/Au [45,46]. As the densely packed Fc reporters could

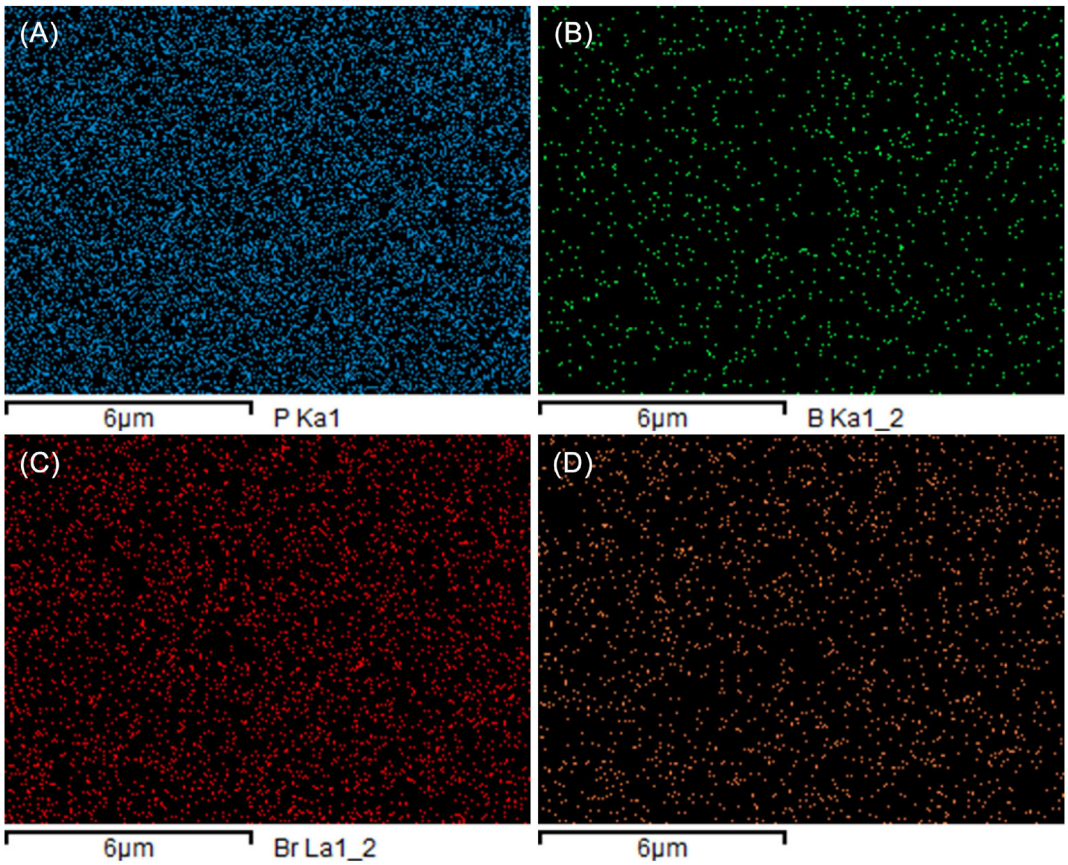

Fig. 4. EDS mappings of (A) P, (B) B, (C) Br, and (D) Fe elements. CEA, 1.0 ng·mL^{-1}.

significantly facilitate the charge transfer between the electrode and the $[Fe(CN)_6]^{3-/4-}$ [38,44,47], the Fc/PBABr/CEA/MH/Apt/Au showed a significantly decreased R_{ct} (Fig. 5A,f) and the significantly increased redox currents (Fig. 5B,f) when compared with the PBABr/CEA/MH/Apt/Au. As the increase of the R_{ct} was accompanied by the decrease of the redox currents, while the decrease of the R_{ct} was accompanied by the increase of the redox currents [48], the EIS results agreed well with the CV results [45,46], which validated the successful preparation of the Fc/PBABr/CEA/MH/Apt/Au.

3.4. Analytical performance of the electrochemical CEA aptasensor

Under the optimal conditions, the analytical performance of the BA-eATRP-based electrochemical CEA aptasensor was investigated. From Fig. 6, it can be seen that the peak current increased with the increase of CEA concentration, indicating

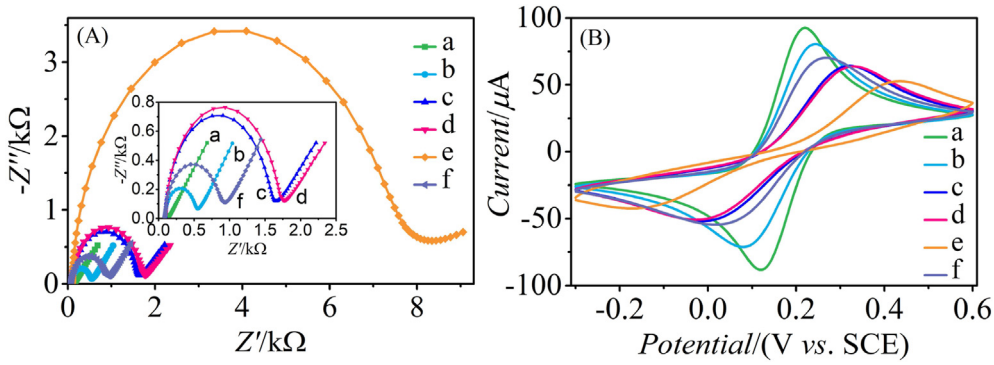

Fig. 5. (A) Nyquist plots and (B) CV curves of the Au (a), Apt/Au (b), MH/Apt/Au (c), CEA/MH/Apt/Au (d), PBABr/CEA/MH/Apt/Au (e), and Fc/PBABr/CEA/MH/Apt/Au (f). CEA, 1.0 ng·mL^{-1}.

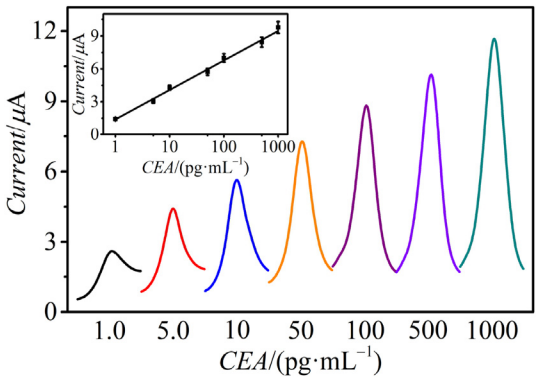

Fig. 6. SWV curves toward various CEA concentrations and the calibration plot (n = 5, *the inset).*

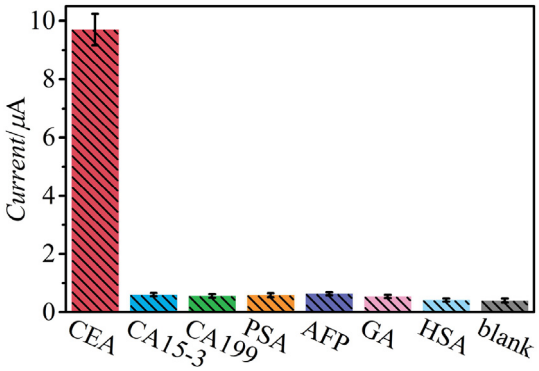

Fig. 7. Peak currents toward 1.0 ng·mL^{-1} CEA or 10 ng·mL^{-1} interferents (n = 5).

the signal-on detection. The inset shows that there was a good linearity between the peak current and the logarithm of CEA concentration over the range from 1.0 to 1000 pg·mL^{-1} (R^2 = 0.995). The regression equation of the calibration plot can be expressed as $y = 1.395 + 2.688\lg x$, in which y represents the peak current in μA and x represents the concentration of CEA in pg·mL^{-1}. The detection limit was calculated to be 0.34 pg·mL^{-1}, which was satisfactory when compared with some of the previous methods (Table S1). The high detection sensitivity was a result of the dual amplification by the BA-eATRP-based strategy. The relative standard deviation (RSD) of the peak current toward the intraassay of 1.0 ng·mL^{-1} CEA was 5.3% (n = 5) while for the interassay it was 5.7% (n = 5), clearly showing that the reproducibility of the electrochemical CEA aptasensor was acceptable. As a proof of concept, the storage of the Fc/PBABr/CEA/MH/Apt/Au at 4 °C for two weeks resulted in the loss of the peak current by about 5.4%, showing the high storage stability of the perfectly modified electrode.

Table 1. Analysis of spiked CEA in human serum.

Sample	Added (pg·mL^{-1})	Found (pg·mL^{-1})	Recovery	RSD (n = 5)
1	1000	943.0	94.3%	5.2%
2	100	103.5	103.5%	5.4%
3	10	10.55	105.5%	5.8%

3.5. Selectivity of the electrochemical CEA aptasensor

The selectivity of the BA-eATRP-based electrochemical CEA aptasensor was investigated based on the detection of 10 ng·mL^{-1} CA15-3, CA199, prostate-specific antigen (PSA), alpha-fetoprotein (AFP), glycated albumin (GA), and human serum albumin (HSA), and 1.0 ng·mL^{-1} CEA. From Fig. 7, it can be seen that the presence of 1.0 ng·mL^{-1} CEA could result in the generation of a high peak current, while the presence of 10 ng·mL^{-1} other component resulted in no significant difference in the intensity of the peak current relative to the blank sample. The results indicated that the BA-eATRP-based electrochemical CEA aptasensor is highly selective. The high selectivity was a result of the aptamer-based recognition [45,46,55–57].

3.6. Analysis of CEA in human serum

The analysis of CEA in human serum was applied to investigate the potential practicability of the BA-eATRP-based electrochemical aptasensor. Due to the lack of clinical specimens, the proof-of-concept experiments were conducted using the commercially supplied NHS. The NHS was filtered using a Millipore Amicon® Ultra-4 centrifugal filter unit (cutoff, 100 kDa) to remove the endogenous CEA antigens, and then diluted by 20 times using 10 mmol·L^{-1} PBS (pH 7.4). As seen in Table 1, the recoveries were within the range from 94.3% to 105.5%, while the RSDs were within the range from 5.2% to 5.8%. The results of the standard addition experiments indicated that the BA-eATRP-based electrochemical aptasensor is applicable to the quantitative analysis of CEA in serum samples.

4. Conclusions

In summary, a cost-effective and easy-to-operate electrochemical aptasensor has been reported for the ultrasensitive and highly selective detection of CEA, taking advantage of the dual amplification by the BA-eATRP. The covalent crosslinking between the PBA group and the *cis*-diol groups of the monosaccharide residues allows for the site-specific labeling of each CEA antigen with hundreds of ATRP initiators, while the surface-initiated growth of long-chain polymers through eATRP results in the tethering of each ATRP initiator-conjugated site with hundreds to thousands of Fc

reporters. Thus, the BA-eATRP enables the labeling of each CEA antigen with a plenty of Fc reporters, leading to the dual-amplification detection. The BA-eATRP-based amplification strategy is free from the use of the sophisticated enzymatic reactions or nanocomposites, offering the benefits of cost-effectiveness and simple operation to the electrochemical aptasensing of CEA. Taking together, the BA-eATRP-based electrochemical CEA aptasensor holds great promise in clinical applications.

Acknowledgements

This work was co-supported by the Guangdong Basic and Applied Basic Research Foundation (No. 2022A1515010618), the Young Talent Support Project of Guangzhou Association for Science and Technology (No. QT-2023-009), the National Natural Science Foundation of China (No. 21904026, 21974031), the Guangzhou Science and Technology Project (No. 202201010600, 202201020170, 20220 1000002), and the Innovation Training Program for College Students of Guangzhou University (No. 202211078113, S202111078031).

References

[1] Fletcher R H. Carcinoembryonic antigen[J]. Ann. Intern. Med., 1986, 104(1): 66−73.
[2] Hall C, Clarke L, Pal A, Buchwald P, Eglinton T, Wakeman C, Frizelle F. A review of the role of carcinoembryonic antigen in clinical practice[J]. Ann. Coloproctol., 2019, 35(6): 294−305.
[3] Benchimol S, Fuks A, Jothy S, Beauchemin N, Shirota K, Stanners C P. Carcinoembryonic antigen, a human tumor marker, functions as an intercellular adhesion molecule[J]. Cell, 1989, 57(2): 327−334.
[4] Huang L T, Zeng Y Y, Liu X L, Tang D P. Pressure-based immunoassays with versatile electronic sensors for carcinoembryonic antigen detection[J]. ACS Appl. Mater. Interfaces, 2021, 13(39): 46440−46450.
[5] Qiu Z L, Shu J, Tang D P. Bioresponsive release system for visual fluorescence detection of carcinoembryonic antigen from mesoporous silica nanocontainers mediated optical color on quantum dot-enzyme-impregnated paper[J]. Anal. Chem., 2017, 89(9): 5152−5160.
[6] Yu Q L, Wang X, Duan Y X. Capillary-based three-dimensional immunosensor assembly for high-performance detection of carcinoembryonic antigen using laser-induced fluorescence spectrometry[J]. Anal. Chem., 2014, 86(3): 1518−1524.
[7] Xing T Y, Zhao J, Weng G J, Zhu J, Li J J, Zhao J W. Specific detection of carcinoembryonic antigen based on fluorescence quenching of hollow porous gold nanoshells with roughened surface[J]. ACS Appl. Mater. Interfaces, 2017, 9(42): 36632−36641.
[8] Fan G C, Zhu H, Du D, Zhang J R, Zhu J J, Lin Y. Enhanced photoelectrochemical immunosensing platform based on CdSeTe@CdS:Mn core-shell quantum dots-sensitized TiO_2 amplified by CuS nanocrystals conjugated signal antibodies[J]. Anal. Chem., 2016, 88(6): 3392−3399.
[9] Guan X X, Deng X X, Song J, Wang X Y, Wu S. Polydopamine with tailorable photoelectrochemical activities for the highly sensitive immunoassay of tumor markers[J]. Anal. Chem., 2021, 93(17): 6763−6769.
[10] Li J J, Zhang Y, Kuang X, Wang Z L, Wei Q. A network signal amplification strategy of ultrasensitive photoelectrochemical immunosensing carcinoembryonic antigen based on CdSe/melamine network as label[J]. Biosens Bioelectron, 2016, 85: 764−770.
[11] Carneiro M C, Sousa-Castillo A, Correa-Duarte M A, Sales M GF. Dual biorecognition by combining molecularly-imprinted polymer and antibody in SERS detection. Application to carcinoembryonic antigen[J]. Biosens. Bioelectron., 2019, 146: 111761.
[12] Chon H, Lee S, Son S W, Oh C H, Choo J. Highly sensitive immunoassay of lung cancer marker carcinoembryonic antigen using surface-enhanced Raman scattering of hollow gold nanospheres[J]. Anal. Chem., 2009, 81(8): 3029−3034.
[13] Wang J, Cao Y, Xu Y Y, Li G X. Colorimetric multiplexed immunoassay for sequential detection of tumor markers[J]. Biosens. Bioelectron., 2009, 25(2): 532−536.
[14] Zhao L J, Wang J, Su D D, Zhang Y Y, Lu H Y, Yan X, Bai J, Gao Y, Lu G Y. The DNA controllable peroxidase mimetic activity of MoS_2 nanosheets for constructing a robust colorimetric biosensor[J]. Nanoscale, 2020, 12(37): 19420−19428.
[15] Zhou Y, Chen S H, Luo X L, Chai Y Q, Yuan R. Ternary electrochemiluminescence nanostructure of Au nanoclusters as a highly efficient signal label for ultrasensitive detection of cancer biomarkers[J]. Anal. Chem., 2018, 90(16): 10024−10030.
[16] Wang N N, Feng Y Q, Wang Y W, Ju H X, Yan F. Electrochemiluminescent imaging for multi-immunoassay sensitized by dual DNA amplification of polymer dot signal[J]. Anal. Chem., 2018, 90(12): 7708−7714.
[17] Yang L, Zhu W, Ren X, Khan M S, Zhang Y, Du B, Wei Q. Macroporous graphene capped Fe_3O_4 for amplified electrochemiluminescence immunosensing of carcinoembryonic antigen detection based on CeO_2@TiO_2[J]. Biosens. Bioelectron., 2017, 91: 842−848.
[18] Wu M S, Shi H W, He L J, Xu J J, Chen H Y. Microchip device with 64-site electrode array for multiplexed immunoassay of cell surface antigens based on electrochemiluminescence resonance energy transfer[J]. Anal. Chem., 2012, 84(9): 4207−4213.
[19] Gu X, She Z, Ma T, Tian S, Kraatz H B. Electrochemical detection of carcinoembryonic antigen[J]. Biosens. Bioelectron., 2018, 102: 610−616.
[20] Ji Y L, Guo J X, Ye B X, Peng G H, Zhang C, Zou L N. An ultrasensitive carcinoembryonic antigen electrochemical aptasensor based on 3D DNA nanoprobe and Exo III[J]. Biosens. Bioelectron., 2022, 196: 113741.
[21] Liang H H, Luo Y, Li Y Y, Song Y H, Wang L. An immunosensor using electroactive COF as signal probe for electrochemical detection of carcinoembryonic antigen[J]. Anal. Chem., 2022, 94(13): 5352−5358.
[22] Hu Q, Ma K F, Mei Y Q, He M H, Kong J M, Zhang X J. Metal-to-ligand charge-transfer: applications to visual detection of β-galactosidase activity and sandwich immunoassay[J]. Talanta, 2017, 167: 253−259.
[23] Wang D F, Li Y Y, Lin Z Y, Qiu B, Guo L H. Surface-enhanced electrochemiluminescence of Ru@SiO_2 for ultrasensitive detection of carcinoembryonic antigen[J]. Anal. Chem., 2015, 87(12): 5966−5972.
[24] Qi J, Li B W, Zhou N, Wang X Y, Deng D M, Luo L Q, Chen L X. The strategy of antibody-free biomarker analysis

by *in-situ* synthesized molecularly imprinted polymers on movable valve paper-based device[J]. Biosens. Bioelectron., 2019, 142: 111533.

[25] Liu Z, Lei S, Zou L N, Li G P, Xu L L, Ye B X. A label-free and double recognition-amplification novel strategy for sensitive and accurate carcinoembryonic antigen assay[J]. Biosens. Bioelectron., 2019, 131: 113−118.

[26] Li J, Xu L Q, Shen Y J, Guo L, Yin H, Fang X H, Yang Z J, Xu Q, Li H B. Superparamagnetic nanostructures for split-type and competitive-mode photoelectrochemical aptasensing[J]. Anal. Chem., 2020, 92(12): 8607−8613.

[27] Zeng X X, Ma S S, Bao J C, Tu W W, Dai Z H. Using graphene-based plasmonic nanocomposites to quench energy from quantum dots for signal-on photoelectrochemical aptasensing[J]. Anal. Chem., 2013, 85(24): 11720−11724.

[28] Zhang Y H, Li M J, Wang H J, Yuan R, Wei S P. Supersensitive photoelectrochemical aptasensor based on Br,N-codoped TiO_2 sensitized by quantum dots[J]. Anal. Chem., 2019, 91(16): 10864−10869.

[29] Ma C, Liu H Y, Zhang L N, Li H, Yan M, Song X R, Yu J H. Multiplexed aptasensor for simultaneous detection of carcinoembryonic antigen and mucin-1 based on metal ion electrochemical labels and $Ru(NH_3)_6^{3+}$ electronic wires[J]. Biosens. Bioelectron., 2018, 99: 8−13.

[30] Yang H Q, Xu Y, Hou Q Q, Xu Q Z, Ding C F. Magnetic antifouling material based ratiometric electrochemical biosensor for the accurate detection of CEA in clinical serum[J]. Biosens. Bioelectron., 2022, 208: 114216.

[31] Zhai X J, Wang Q L, Cui H F, Song X, Lv Q Y, Guo Y. A DNAzyme-catalyzed label-free aptasensor based on multifunctional dendrimer-like DNA assembly for sensitive detection of carcinoembryonic antigen[J]. Biosens. Bioelectron., 2021, 194: 113618.

[32] Wang Q L, Cui H F, Song X, Fan S F, Chen L L, Li M M, Li Z Y. A label-free and lectin-based sandwich aptasensor for detection of carcinoembryonic antigen[J]. Sens. Actuators, B, 2018, 260: 48−54.

[33] Paniagua G, Villalonga A, Eguílaz M, Vegas B, Parrado C, Rivas G, Díez P, Villalonga R. Amperometric aptasensor for carcinoembryonic antigen based on the use of bifunctionalized Janus nanoparticles as biorecognition-signaling element[J]. Anal. Chim. Acta, 2019, 1061: 84−91.

[34] Guo C P, Su F F, Song Y P, Hu B, Wang M H, He L H, Peng D L, Zhang Z H. Aptamer-templated silver nanoclusters embedded in zirconium metal-organic framework for bifunctional electrochemical and SPR aptasensors toward carcinoembryonic antigen[J]. ACS Appl. Mater. Interfaces, 2017, 9(47): 41188−41199.

[35] Wu Y F, Liu S Q, He L. Electrochemical biosensing using amplification-by-polymerization[J]. Anal. Chem., 2009, 81(16): 7015−7021.

[36] Yuan L, Wei W, Liu S Q. Label-free electrochemical immunosensors based on surface-initiated atom radical polymerization[J]. Biosens. Bioelectron., 2012, 38(1): 79−85.

[37] He P, Zheng W, Tucker E Z, Gorman C B, He L. Reversible addition-fragmentation chain transfer polymerization in DNA biosensing[J]. Anal. Chem., 2008, 80(10): 3633−3639.

[38] Hu Q, Han D X, Gan S Y, Bao Y, Niu L. Surface-initiated-reversible-addition−fragmentation-chain-transfer polymerization for electrochemical DNA biosensing[J]. Anal. Chem., 2018, 90(20): 12207−12213.

[39] Wu Y F, Wei W, Liu S Q. Target-triggered polymerization for biosensing[J]. Acc. Chem. Res., 2012, 45(9): 1441−1450.

[40] Hu Q, Gan S Y, Bao Y, Zhang Y W, Han D X, Niu L. Controlled/"living" radical polymerization-based signal amplification strategies for biosensing[J]. J. Mater. Chem. B, 2020, 8(16): 3327−3340.

[41] Wang J S, Matyjaszewski K. Controlled/"living" radical polymerization. Atom transfer radical polymerization in the presence of transition-metal complexes[J]. J. Am. Chem. Soc., 1995, 117(20): 5614−5615.

[42] Magenau A J, Strandwitz N C, Gennaro A, Matyjaszewski K. Electrochemically mediated atom transfer radical polymerization[J]. Science, 2011, 332(6025): 81−84.

[43] Hu Q, Wang Q W, Sun G Z, Kong J M, Zhang X J. Electrochemically mediated surface-initiated de novo growth of polymers for amplified electrochemical detection of DNA [J]. Anal. Chem., 2017, 89(17): 9253−9259.

[44] Hu Q, Gan S Y, Bao Y, Zhang Y W, Han D X, Niu L. Electrochemically controlled ATRP for cleavage-based electrochemical detection of the prostate-specific antigen at femtomolar level concentrations[J]. Anal. Chem., 2020, 92(24): 15982−15988.

[45] Hu Q, Hu S H, Li S Q, Liu S J, Liang Y Y, Cao X J, Luo Y L, Xu W J, Wang H C, Wan J W, Feng W X, Niu L. Boronate affinity-based electrochemical aptasensor for point-of-care glycoprotein detection[J]. Anal. Chem., 2022, 94(28): 10206−10212.

[46] Hu Q, Wan J W, Wang H C, Cao X J, Li S Q, Liang Y Y, Luo Y L, Wang W, Niu L. Boronate-affinity cross-linking-based ratiometric electrochemical detection of glycoconjugates[J]. Anal. Chem., 2022, 94(26): 9481−9486.

[47] Hu Q, Su L F, Chen Z H, Huang Y Y, Qin D D, Niu L. Coenzyme-mediated electro-RAFT polymerization for amplified electrochemical interrogation of trypsin activity [J]. Anal. Chem., 2021, 93(27): 9602−9608.

[48] Hu Q, Su L F, Luo Y L, Cao X J, Hu S H, Li S Q, Liang Y Y, Liu S J, Xu W J, Qin D D, Niu L. Biologically mediated RAFT polymerization for electrochemical sensing of kinase activity[J]. Anal. Chem., 2022, 94(16): 6200−6205.

[49] Fu Z F, Liu H, Ju H X. Flow-through multianalyte chemiluminescent immunosensing system with designed substrate zone-resolved technique for sequential detection of tumor markers[J]. Anal. Chem., 2006, 78(19): 6999−7005.

[50] Zhou L L, Wang Y J, Xing R R, Chen J, Liu J, Li W, Liu Z. Orthogonal dual molecularly imprinted polymer-based plasmonic immunosandwich assay: A double characteristic recognition strategy for specific detection of glycoproteins [J]. Biosens. Bioelectron., 2019, 145: 111729.

[51] Wu X, Li Z, Chen X X, Fossey J S, James T D, Jiang Y B. Selective sensing of saccharides using simple boronic acids and their aggregates[J]. Chem. Soc. Rev., 2013, 42(20): 8032−8048.

[52] Zhang W, Liu W, Li P, Xiao H B, Wang H, Tang B. A fluorescence nanosensor for glycoproteins with activity based on the molecularly imprinted spatial structure of the target and boronate affinity[J]. Angew. Chem. Int. Ed., 2014, 53(46): 12489−12493.

[53] Li D J, Chen Y, Liu Z. Boronate affinity materials for separation and molecular recognition: structure, properties and applications[J]. Chem. Soc. Rev., 2015, 44(22): 8097−8123.

[54] Ye J, Chen Y, Liu Z. A boronate affinity sandwich assay: An appealing alternative to immunoassays for the determination of glycoproteins[J]. Angew. Chem. Int. Ed., 2014, 53(39): 10386−10389.

[55] Wu L L, Wang Y D, Xu X, Liu Y L, Lin B Q, Zhang M X, Zhang J L, Wan S, Yang C Y, Tan W H. Aptamer-based detection of circulating targets for precision medicine[J]. Chem. Rev., 2021, 121(19): 12035−12105.

[56] Tan W, Donovan M J, Jiang J. Aptamers from cell-based selection for bioanalytical applications[J]. Chem. Rev., 2013, 113(4): 2842−2862.

[57] Zhu Z, Song Y, Li C, Zou Y, Zhu L, An Y, Yang C J. Monoclonal surface display SELEX for simple, rapid, efficient, and cost-effective aptamer enrichment and identification[J]. Anal. Chem., 2014, 86(12): 5881−5888.

基于硼酸盐亲和辅助电化学调控 ATRP 的癌胚抗原超灵敏电化学适体传感研究

胡　琼*，李诗琪，梁伊依，冯文星，骆怡琳，曹晓静，牛　利*
广州大学化学化工学院，广东省光电传感材料与器件工程技术研究中心，广州市传感材料与器件重点实验室，广州大学分析科学技术研究中心，广东 广州 510006

摘要

癌胚抗原（CEA）是一种酸性糖蛋白，其作为一种广谱肿瘤标志物在恶性肿瘤的鉴别诊断与监测等方面具有重要价值。在此，借助于硼酸盐亲和辅助电化学调控原子转移自由基聚合（BA-eATRP）的双重信号放大作用，我们报道了一种电化学适体传感器，用于 CEA 的超灵敏、高选择性检测。基于 BA-eATRP 的电化学 CEA 适体传感的基本原理为：待核酸适体捕获 CEA 抗原后，借助于苯硼酸（PBA）基团与单糖残基上的顺式二醇基团间的选择性亲和相互作用将 ATRP 引发剂位点靶向性地共价偶联到 CEA 抗原上；随后，以二茂铁甲基丙烯酸甲酯（FcMMA）作为单体，借助于 eATRP 将二茂铁（Fc）探针引入电极表面。由于 CEA 上含有数百个顺式二醇基团，基于硼酸盐亲和的交联反应可使得在每个 CEA 抗原上标记数百个 ATRP 引发剂分子。此外，通过 eATRP 反应，可以在电极表面接枝长的二茂铁基聚合物链，使得每个标记有 ATRP 引发剂的位点均能连接上成百上千个 Fc 探针。因此，BA-eATRP 可使得每个 CEA 抗原上标记上大量的 Fc 探针。在最佳条件下，基于 BA-eATRP 的电化学适体传感器能够实现浓度低为 0.34 pg·mL^{-1} 的 CEA 的高选择性检测，其线性范围为 1.0–1000 pg·mL^{-1}。而且，该适体传感器可用于人血清中 CEA 的定量分析。基于 BA-eATRP 的电化学适体传感器具有成本低廉、操作简便等优良特性，在 CEA 的超灵敏、高选择性检测方面具有广阔的应用前景。

关键词：硼酸盐亲和；原子转移自由基聚合；电化学适体传感器；癌胚抗原；肿瘤标志物；信号放大